Наносистеми, наноматеріали, нанотехнології
Nanosistemi, Nanomateriali, Nanotehnologii
2023, т. 21, № 2, сс. 253–260

PACS numbers: 71.70.Ej, 76.30.Fc, 78.55.Et, 81.07.Wx, 81.15.Gh, 81.70.Jb, 82.80.Ms

Temperature Behaviour of the EPR Spectrum of Polycrystalline ZnSe

I. I. Abbasov

Azerbaijan State Oil and Industry University,
20, Azadlig Str.,
1010 Baku, Azerbaijan

The temperature behaviour of the EPR spectrum of polycrystalline ZnSe, which is characteristic of bivalent Jahn–Teller copper ions Cu^{++}, is studied. The temperature dependence of the EPR spectra shows a decrease in the EPR-spectrum linewidth from 300 K to 120 K, but, at a temperature below 120 K, the EPR lines are broaden. This broadening can be associated with the transition of the bivalent ion Cu^{++} to the univalent state.

Вивчено температурну поведінку спектру ЕПР полікристалічного ZnSe, характерну для двовалентних йонів Купруму Cu^{++} Яна–Теллера. Температурна залежність спектрів ЕПР показує зменшення ширини лінії ЕПР-спектру від 300 К до 120 К, але за температури нижче 120 К лінії ЕПР розширюються. Це розширення може бути пов'язане з переходом двовалентного йона Cu^{++} у одновалентний стан.

Key words: EPR in polycrystalline ZnSe, Jahn–Teller effect, ions Cu^{++}, magnetic phase transitions, tetragonally distorted octahedrons.

Ключові слова: ЕПР в полікристалах ZnSe, ефект Яна–Теллера, йони Cu^{++}, магнетні фазові переходи, тетрагонально спотворені октаедри.

(Received 18 September, 2022)

1. INTRODUCTION

In recent years, the role of oxygen and the influence of the sample surface on the optical properties of $A_{II}B_{VI}$ crystals, including the luminescence processes observed in these materials, have been intensively studied [1–10]. This is because the long-wavelength emission bands observed in these crystals are impurity-defect luminescence spectra, the study of the properties of which is necessary for

modern optoelectronics operating in the blue-green and red regions of the spectrum [1, 4]. In Refs. [6–10], where photoluminescence has been studied from a polished and unpolished sample surface (in both cases, in the same sample, there is the same excitation); some difference has been observed in the spectra, and it was considered that this difference is due to the uneven distribution of background impurities (they can be called uncontrolled impurities) over the depths of the sample. The temperature behaviour of the intensity of the green band under UV excitation (325 nm), observed from the polished and unpolished sample surfaces in the temperature range of 80–180 K, is different, and a similar behaviour has been observed upon excitation by x-rays, where the quantum energy is of 12 keV [6, 8]. The authors of Refs. [4, 11] assume that the yellow–green luminescence of polycrystalline CVD ZnSe is due to the transition of electrons from a shallow donor to an associative acceptor centre, which includes O and Cu background impurities $\{Cu^{+}O(Se)\}$. For volume and charge compensation of the isoelectronic acceptor OSe, the incorporation of Cu ensures the formation of a stable complex $\{Cu_{Zn}^{++}–Cu^{+}O(Se)\}$ called an associative acceptor centre, *i.e.*, it is assumed that Cu can be in two charge states in the sample under study. As also known, the yellow–green luminescence is associated with Cu^{++} ($3d^9$) ions, and the red one is associated with Cu^{+} ($3d^{10}$).

The change in the concentration of copper ions as a function of temperature in the polycrystalline CVD ZnSe sample under study is very important for investigating the intensity of the observed luminescence in the blue–green and red regions of the spectrum. Therefore, in this paper, we want to study the temperature behaviour of the EPR spectrum, since Cu^{++} ($3d^9$) ions have unpaired electrons, *i.e.*, must have paramagnetic properties.

2. METHODS AND EXPERIMENTS

Polycrystalline ZnSe samples with the thicknesses of 3 mm were obtained with a chemical-vapour deposition method (CVD). In the CVD method, the crystal growth from the vapour phase occurs at a lower temperature compared to the melting technology, which helps to reduce the concentration of bulk defects, and reduces the contamination of the growing crystal with the ampoule material. Concentration of background impurities for the polycrystalline CVD ZnSe sample under study was determined by two methods: atomic emission spectroscopy and laser mass spectrometry. The total impurity content is of $< 10^{16}–10^{17}$ cm^{-3} ($\cong 10^{16}$ cm^{-3} of Cu). Oxygen concentration is controlled by chemical gas chromatographic analysis and is of $\cong 10^{18}–10^{20}$ cm^{-3}.

In the given paper, the study of the EPR spectra of polycrystal-

line CVD ZnSe in the temperature range of 108–300 K was carried out with an Elexsys 580 spectrometer (manufactured by Bruker), operating at a frequency of 9.4348 GHz (x-band) with a magnetic field modulation frequency of 100 kHz. The sensitivity of the device is of $1.2 \cdot 10^9$ spin/g. The first derivative of the EPR absorption line was recorded in the temperature range of 108–300 K. The number of paramagnetic electrons was calculated from a comparison of the EPR spectra of the test and reference samples ($T = 300$ K) and has a value of the order of $\cong 3 \cdot 10^{17}$.

The diffraction pattern of the CVD ZnSe sample was taken using a Miniflex 600 x-ray diffractometer (XRD). To study the morphology and microcomposition of the sample surface, a Japanese-made scanning electron microscope JEOL JSM6610-LV was used.

3. X-RAY STRUCTURAL ANALYSIS AND OPTICAL MICROSCOPY

The diffraction pattern of the ZnSe sample obtained by chemical vapour deposition is shown in Fig. 1. According to the results of x-ray phase analysis of the studied sample, zinc selenide is polycrystalline, and analysis of the x-ray reflection intensity shows the presence of a predominant direction in the crystal, as well as the

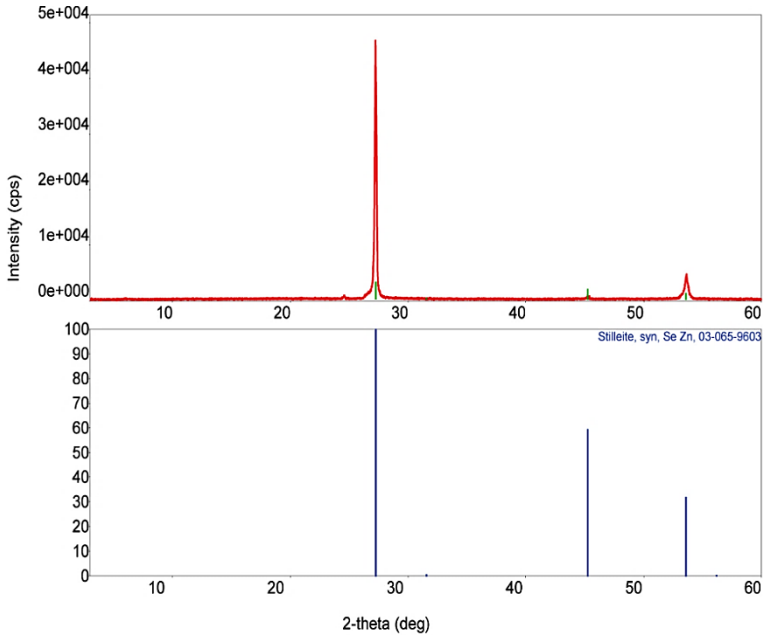

Fig. 1. X-ray diffraction in CVD ZnSe.

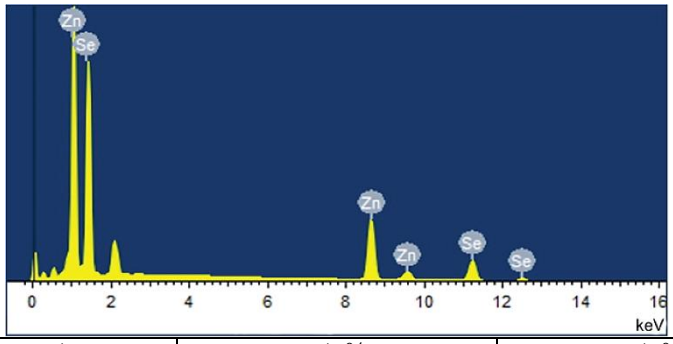

Element	wt.%	at.%
Zn*K*	44.08	48.78
Se*L*	55.92	51.22

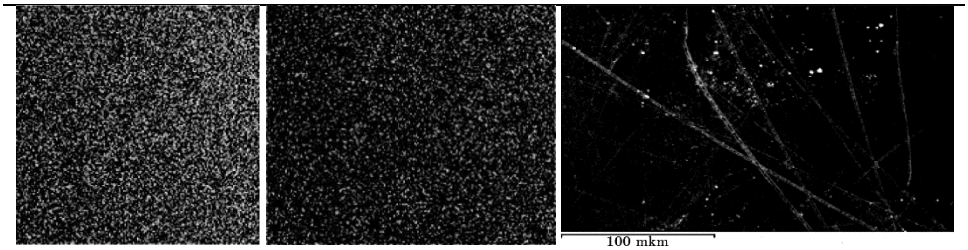

ZnK_{α_1} SeK_{α_1}

Fig. 2. X-ray microanalysis and micrographs of the CVD ZnSe crystal surface.

fact that the sample consists of single phase, *i.e.*, cubic phase with sphalerite structure (space group $F43m$ (T_d^2), face-centred cubic lattice), with lattice parameter $a_0 = 5.667$ Å. The data obtained correspond to the previously known results [12]. Quantitative x-ray microanalysis determines the phase composition and the distribution of chemical elements on the sample surface under study (Fig. 2).

Analysis of the obtained results shows the surface homogeneity, but with a change in stoichiometry within the ZnSe homogeneity region towards an excess of selenium (Fig. 2) [6].

4. EPR STUDIES: RESULTS AND DISCUSSIONS

The observed EPR spectra are characteristic of bivalent Jahn–Teller copper ions Cu^{++} (Fig. 3). This conclusion is made from the determination of the g-factors and the observation of hyperfine splitting due to the interaction with the copper own magnetic core.

The absorbed energy is proportional to the total number of unpaired electrons in the sample under study. The resonance linewidth ΔH was determined as the distance between the values of the mag-

netic field, at which the first derivative of the absorption line reaches its minimum and maximum values. The temperature dependence of the linewidth of the central component of the EPR spectrum is shown in Table.

As can be seen (Fig. 3) at room temperature ($T = 300$ K), the anisotropy of the g-tensor and the anisotropy of the A-tensor are absent, and the anisotropy is observed at $T = 140$ K. To estimate the anisotropy of the g-tensor and the anisotropy of the A-tensor (hyperfine interaction tensor), calculations were carried out in the package [13]. It is obtained that $g_{\parallel} = 2.5$, $g_{\perp} = 2.12$ and $A_{\parallel} = 0.08$ cm^{-1}, $A_{\perp} \leq 0.005$ cm^{-1} and, with decreasing temperature to 108 K, the anisotropy of the g-tensor does not change. The calculated EPR spectrum at $T = 140$ K is shown in Fig. 3 by a dotted line. $g_{\parallel} > g_{\perp} > g_e$,

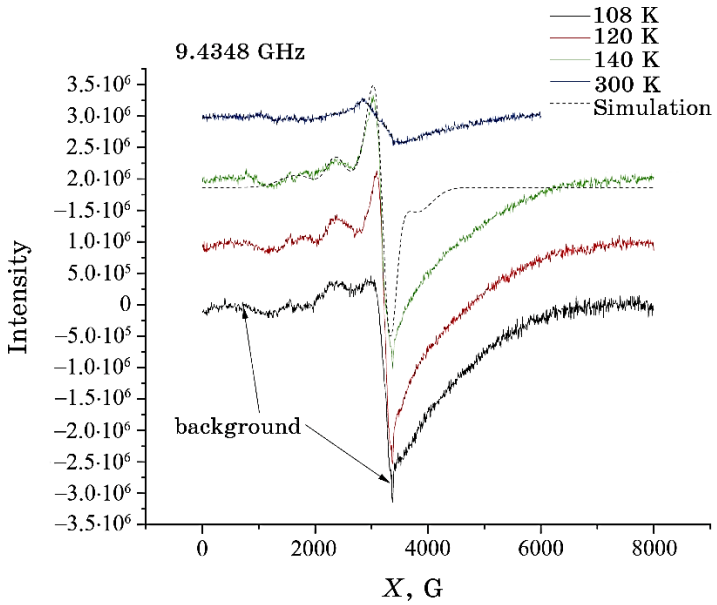

Fig. 3. Temperature dependence of the EPR spectrum of polycrystalline ZnSe.

TABLE. Temperature dependence of the linewidth ΔH of the central component of the EPR spectrum.

Temperature, K	Linewidth, G
300	560
140	350
120	290
108	390

where $g_e = 2.0023$ is g-factor for free electron. Consequently, from the values of g and the shape of the EPR spectra, it can be concluded that the ground state of Cu^{++} ions is the $d_{x^2-y^2}$ orbital, and Cu^{++} ions are located in tetragonally distorted octahedral positions [14, 15]. The ratio $(g_\parallel - g_e)/(g_\perp - g_e)$, which determines the position of the unpaired electron of the Cu^{++} ion, also confirms that the ground state for Cu^{++} ions is $d_{x^2-y^2}$ (state $2B1g$) [15, 16].

It can be suggested that, as a result of the interaction of Cu ions with oxygen ligands, an oxygen octahedron is formed, which is elongated in a distorted tetragonal order with elongation per molecule in the direction of the Z-axis. The ratio $g_\parallel/A_\parallel$ determines the degree of this distortion [16]. In our case, the ratio $g_\parallel/A_\parallel$ is equal to $\cong 30$ and is quite small compared to 200. Usually, large values of $g_\parallel/A_\parallel$ are due to the tetragonal distortion caused by the introduction of a ligand with a weaker crystal field [16]. Therefore, it can be asserted that, in our case, the Jahn–Teller tetragonal distortions are caused by the introduction of a ligand with a stronger crystal field. It is known that the electronic configuration of the Cu^{++} ion in an octahedral environment with Jahn–Teller tetragonal distortion can be an extended or compressed octahedron, where the ground state of the Cu^{++} ions in compressed octahedral sites is the d_{z^2} orbital. Since there is only one electron in the $d_{x^2-y^2}$ orbital, the Cu^{++}-ligand bond is stronger due to these electrons than due to d_{z^2} electrons. This change reduces the total energy, since the energy of two electrons in the d_{z^2} orbital decreases, and the energy of one electron in the $d_{x^2-y^2}$ orbital increases. On the other hand, in elongated tetragonally distorted octahedral sites, four ligands in the xy-plane are bonded to the Cu^{++} ion more strongly than two ligands located along the z-axis and, depending on this one, the degree of distortion in Cu^{++} complexes is different.

From the temperature dependence of the EPR spectra, a decrease in the line width in the EPR spectrum from 300 K to 120 K is observed. It is known that the width of the EPR spectrum depends on the interaction of the magnetic moment of an electron with the magnetic moments of the surrounding nuclei (lattice) and electrons [17] and usually decreases with decreasing temperature, which is associated with a decrease in the spin relaxation rate. At temperatures below 120 K, broadening of the EPR lines is observed (Fig. 3). This broadening can be attributed with the transition processes of the bivalent copper ion (Cu^{++}) to the monovalent state (Cu^{+}), *i.e.*, a magnetic phase transition occurs.

Magnetic phase transitions for copper ions at $T < 130$ K are observed not only in ZnSe and even earlier were observed in copper-carbon compounds [18], and, in this case, the width of magnetic phase transitions for copper ions is estimated to be $\Delta T = 30$ K.

We suppose that in our case at least two types of centres are also

formed, which are due to different charges and, accordingly, nonmagnetic states of copper in the $3d^{10}$ (Cu^{+}) configuration and magnetic states in $3d^{9}$ (Cu^{++}). The modification of copper states occurs with the direct participation of oxygen, *i.e.*, with the help of oxygen bridges forming the Cu^{++} magnetic state.

For volume and charge compensation of the isoelectronic acceptor O(Se), the incorporation of copper in the form of Cu_{Zn}^{++}–Cu^{+}, where Cu^{++} ($3d^{9}$) ions replace zinc at lattice sites and Cu^{+} ($3d^{10}$) at interstices, ensures the formation of a stable complex {Cu_{Zn}^{++}–Cu^{+}O(Se)}, called an associative acceptor centre.

The bond of copper ions Cu^{++} ($3d^{9}$) with oxygen is ionic, but, with Cu^{+} ($3d^{10}$), it is covalent. Up to a temperature of 130 K, the ionic bond predominates, and, at $T < 130$ K, the covalent bond of the copper ion with the surrounding oxygen atoms is significant, *i.e.*, as the distance between Cu and oxygen decreases, the covalence increases [18–20]. Thus, copper in the CVD ZnSe sample can be in the region of transition from ionic to covalent bonds; this is also indicated by the large value of the HFS constant $A_{\|} = 0.08$ cm^{-1}.

The formation of two charge states of copper (Cu^{++}, Cu^{+}) in polycrystalline CVD ZnSe depending on the temperature and the action of a different type of excitation source are necessary for a more detailed study of luminescence processes in the yellow–green and red regions of the spectrum, in which the observation of such processes in the spectra is directly related to presence of copper and oxygen.

5. CONCLUSIONS

Based on *g*-values and the shape of the EPR spectra, it was concluded that the ground state of the Cu^{++} ions is the $d_{x^2-y^2}$ orbital, while the Cu^{++} ions are located in tetragonally distorted octahedral positions. This position of the Cu^{++} ion is retained when the temperature is lowered to 120 K. However, at temperatures below 120 K, due to the magnetic phase transition, the bivalent copper ion (Cu^{++}) passes into the univalent nonmagnetic state (Cu^{+}).

The results of this work can be used for a more detailed study of luminescence processes in the yellow–green and red regions of the spectrum, in which the observation of such spectra in $A_{II}B_{VI}$ compounds is directly related to the presence of copper and oxygen in the composition.

REFERENCES

1. V. I. Gavrilenko, A. M. Grekhov, D. V. Korbutyak, and V. G. Litovchenko, *Opticheskie Svoistva Poluprovodnikov: Spravochnik* [Optical Properties of

Semiconductors: Handbook] (Kiev: Naukova Dumka: 1987) (in Russian).
2. W. Walukiewicz, W. Shan, K. M. Yu, J. W. Ager III, E. E. Haller, I. Miotkowski, M. J. Seong, H. Alawadhi, and A. K. Ramdas, *Phys. Rev. Lett.*, **85**: 1552 (2000); https://doi.org/10.1103/PhysRevLett.85.1552
3. K. M. Yu, W. Walukiewicz, J. Wu, W. Shan, J. W. Beeman, M. A. Scarpulla, O. D. Dubon, and P. Becla, *Phys. Rev. Lett.*, **91**: 246403 (2003); https://doi.org/10.1103/PhysRevLett.91.24640
4. N. K. Morozova, *New in the Optics II{VI{O Compounds* (Riga, Latvia: LAP LAMBERT Academic Publishing: 2021).
5. N. K. Morozova and I. I. Abbasov, *Fiz. Tekhn. Poluprovod.*, **56**, No. 5: 463 (2022); doi:10.21883/FTP.2022.05.52350.9793
6. I. Abbasov, M. Musayev, J. Huseynov, E. Gavrishuk, S. Asadullayeva, A. Rajabli, and D. Askerov, *Int. J. Mod. Phys. B*, **36**, No. 02: 2250018 (2022); https://doi.org/10.1142/S0217979222500187
7. I. Abbasov, M. Musayev, J. Huseynov, M. Kostyrko, S. Babayev, G. Eyyubov, and S. Aliyeva, *Ukr. J. Phys. Opt.*, **21**, No. 2: 103 (2020); doi:10.3116/16091833/21/2/103/2020
8. I. Abbasov, M. Musayev, J. Huseynov, M. Kostyrko, G. Eyyubov, and D. Askerov, *Ukr. J. Phys. Opt.*, **21**, No. 3: 159 (2020); doi:10.3116/16091833/21/3/159/2020
9. B. L. Abrams and P. H. Holloway, *Chem. Rev.*, **104**, No. 12: 5783 (2004); https://doi.org/10.1021/cr020351r
10. J. A. Garcia, A.Remyn, A. Zubiaga, V.Mucoz-Sanjosé, and C. Martinez-Tomás, *phys. stat. sol. (a)*, **194**, No. 1: 338 (2002); https://doi.org/10.1002/1521-396X(200211)194:1<338::AID-PSSA338>3.0.CO;2-D
11. G. N. Ivanova, V. A. Kasiyan, D. D. Nedeoglo, and S. V. Oprya, *Semiconductors*, **32**, No. 2: 154 (1998); https://doi.org/10.1134/1.1187337
12. D. D. Nedeoglo and A. V. Simashkevich, *Ehlektricheskie i Lyuminestsentnyye Svoistva Selenida Tsinka* [Electric and Luminescent Properties of Zinc Selenide] (Kishinev: Shtiintsa: 1984) (in Russian).
13. S. Stoll and A. Schweiger, *J Magn. Reson.*, **178**, No. 1: 42 (2006); https://doi.org/10.1016/j.jmr.2005.08.013
14. R Ajay Kumar, M. V. V. K. Srinivas Prasad, G. Kiran Kumar, M. Venkateswarlu, and Ch. Rajesh, *Phys. Scr.*, **94**: 115806 (2019); https://doi.org/10.1088/1402-4896/ab242a
15. B. Sumalatha, I. Omkaram, T. Rajavardhana Rao, and Ch. Linga Raju, *J. Non-Cryst. Solids*, **357**, Nos. 16–17: 3143 (2011); http://dx.doi.org/10.1016/j.jnoncrysol.2011.05.005
16. P. Geetha, K. Parthipan, P. Sathya, and S. Balaji, *Asian J. Chem.*, **25**, No. 9: 4791 (2013); doi:10.14233/ajchem.2013.14104
17. A. Abragam and B. Bleaney, *Electron Paramagnetic Resonance of Transitions* (Oxford, England: Oxford University Press: 1970).
18. B. P. Popov, *Fiz. Tekhn. Poluprovod.*, **39**, No. 4: 479 (2005) (in Russian).
19. M. Purnima, Avula Edukondalu, K. Siva Kumar, and Syed Rahman, *Mat. Res.*, **20**, No. 1: 46 (2017); http://dx.doi.org/10.1590/1980-5373-MR-2016-0042
20. Rajesh Kumar Sharma and V. Ilamathi, *Asian J. Chem.*, **30**, No. 4: 841 (2018); doi:10.14233/ajchem.2018.21081